MICRO-STREAMING CHARACTERISATION IN SHORT PATH LENGTH STANDING WAVE CHAMBERS

L.A. Kuznetsova*, C.J. Bates# and W.T. Coakley*
* School of Biosciences, Cardiff University, UK
#School of Engineering, Division of Mechanical Engineering, Cardiff University, UK
KuznetsovaL@cf.ac.uk

Abstract

Micro-streaming induced in cylindrical and rectangular resonators with 1/2 and 1/4 wavelength (λ) channel depth (acoustic path length) has been monitored non-invasively by microscopic observation of 1.0 μm diameter fluorescent latex tracer particles. The velocity fields were characterised by Particle Image Velocimetry (PIV).

The streaming pattern in a cylindrical resonator with a fixed λ/2 channel depth was consistent with the model described by Rayleigh [1]. The acoustic fields of a rectangular and a cylindrical resonator with a variable channel depth presented patterns characteristic of complex acoustic pressure distribution. Normally, two layers of concentrated tracer particles were observed. Vortices of different spatial scales were also present. It is argued that the redistribution of particles in the vortices is due to the non-uniformity in the acoustic pressure field.

Introduction

Suspended particles in ultrasonic standing waves (USWs) first of all are affected by the direct acoustic radiation force (DRF) [2]. The stronger, axial component, drives particles towards either a pressure node or an anti-node plane (depending on the acoustic properties of the suspension), whereas the lateral components, which are about two orders of magnitude smaller, act within the planes and contribute to the lateral concentration into "clumps".

Ultrasonic resonators may be fabricated so that the depth of the chamber (acoustic path length in the resonator) is equal to either λ/2 or λ/4. The only acoustic pressure node occurs either in the centre of the chamber or at the surface of the reflector, respectively. Ideally, suspended particles are expected to be driven to those positions and to concentrate in a monolayer [3].

USWs also cause acoustic streaming – non-oscillatory steady fluid motion originating from the spatial non-uniformity of the sound field or from energy dissipation at the liquid-solid interfaces of the container. The following classification of streaming is generally accepted [4]:

- Eckart streaming, which results from the attenuation of the wave in the bulk fluid; the scale of the streaming is much greater than λ;
- Schlichting micro-streaming is a vortex flow inside the thin boundary layer at a solid-liquid interface caused by energy losses; the scale of the streaming is much smaller than λ;
- Rayleigh micro-streaming is a vortex flow outside the boundary layer; the scale of the streaming is of the same order of magnitude as λ.

Rayleigh carried out the first theoretical study of streaming when he treated the case of standing waves between parallel walls [1]. Comprehensive reviews on acoustically induced flow are now available [4,5]. New experimental approaches to monitoring acoustic streaming have become possible due to the development of optical flow visualisation techniques, PIV in particular [6]. It has been demonstrated that acoustically generated streaming may find its application in processes such as heat transfer [7] or DNA hybridization rate enhancement [8]. It can also be utilised in medical diagnostics [9].

In the present work acoustic micro-streaming and its effect on particle concentration in short path length mini-chambers have been studied.

Methods

The chambers are based on three main features: an ultrasonic transducer, a spacer and a glass reflector [3]. A coupling stainless steel layer to which a transducer was glued separated the latter from the water layer.

The 12 mm diameter disc transducers' nominal resonance frequency was 1.5 MHz for the cylindrical chambers. Each transducer's back electrode was etched to produce an active radiation area of 8 mm in diameter. The fixed channel depth of one cylindrical chamber was 0.5 mm, which is equivalent to λ/2 at 1.5 MHz (Fig. 1a). The screw-top and elastic o-ring gasket of the second cylindrical chamber allowed continuous variation of the channel depth from 0.5 mm (λ/2) to 0.25 mm (λ/4) (Fig 1b).

The transducer of a rectangular resonator had a nominal thickness resonance frequency of 3 MHz. The active radiation area was 20×10 mm^2. The channel's area was 51×10 mm^2. Brass spacers of 125 and 250 μm thick provided options for the channel depths (Fig. 1c).

An HP function synthesizer provided a sine wave input to an ENI 2100L amplifier. Frequency and applied voltage was controlled by computerised

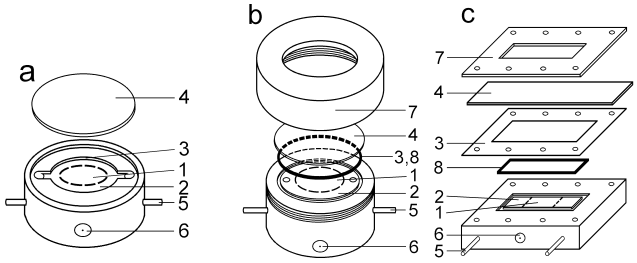

Figure 1. Design of mini-chambers: (a) cylindrical with fixed water layer depth, (b) cylindrical with variable water depth, (c) rectangular; 1– piezoelectric transducer's area, 2– steel layer, 3– spacer for water layer, 4– glass reflector, 5– water inlet (outlet), 6– electrical connection, 7– screw-top (top brass), 8– elastic gasket (o-ring).

tracking of the driving frequency. The software STAND developed at Cardiff University scans the voltage-frequency spectra from a voltmeter and allows the frequency to be held either at voltage maximum or minimum. A function generator (HM 8130, HAMEG Instruments), also used in the experiments, allowed both the maintenance of fixed ultrasonic conditions during the experiment and the gradual variation of the parameters of the sound field.

Polystyrene plain latex beads of 24 μm diameter and fluorescent 1.0 μm latex (Polysciences) were used for the characterisation of the sound field pressure amplitude and for flow visualization, respectively.

The observation of particle movement was carried out with an Olympus BX41M epi-fluorescent microscope. A Fujitsu video camera was connected via a 0.5 microscope adaptor and the images were recorded onto a standard video tape. The recorded video sequences were transferred to a PC video card in digital format with hardware MJPEG data compression (Pinnacle Miro Video DC30+) to be further processed with PIV software.

Two software packages were used for the estimation of velocity fields: PIV Sleuth developed by K.T.Christensen, S.M.Soloff and R.J.Adrian, University of Illinois and FlowManager developed by Dantec Dynamics (Denmark).

The acoustic pressure amplitude was estimated from the balance of the DRF_a and gravitational force acting on a particle in suspension [3]. Linear extrapolation of the pressure at the threshold voltage to the voltage applied in experiment provided acoustic pressure amplitude values for particular drive conditions.

Electrical admittance of the chambers was measured using an Agilent Technologies Network Analyser (HP 8753E).

Results and Discussion

Cylindrical chamber with fixed channel depth

The cylindrical mini-chamber used in this work (channel depth of 0.5 mm, Fig. 1a), had one central pressure node plane. Frequency-voltage spectra showed a resonance at ~1.38 MHz, which was close to the transducer's thickness resonance and was maintained in experiments by the Hameg wave generator. When ultrasound was applied, 24 μm latex particles, driven by the axial and lateral direct radiation forces, concentrated in a single clump near the centre of the chamber in the only pressure node.

The behaviour of small (1.0 μm) latex beads was different since they are relatively more affected by streaming than are bigger particles [3]. When ultrasound was switched on, the particles driven by the axial direct radiation force came to the pressure node plane, at which the microscope was pre-focused, within 0.2 s and then moved from the central source point towards the periphery of the chamber. After a few seconds they concentrated at the edge of the active radiation area of about 6 mm in diameter, not entering the central space again. Apparently, at first following the streaming in the pressure node plane, the particles reached the area where, according to the Rayleigh theory, the velocity of streaming in the lateral direction was negligible, and were then held there by the axial DRF_a [3]. The experiment was repeated at different acoustic pressures. The velocities of the particles in the pressure node plane increased with the increase of acoustic pressure in the system. Fig. 2 displays the velocity field in the pressure node plane after the beginning of sonication. For all the validated vectors, in this chamber, the standard error of the mean did not exceed 10%.

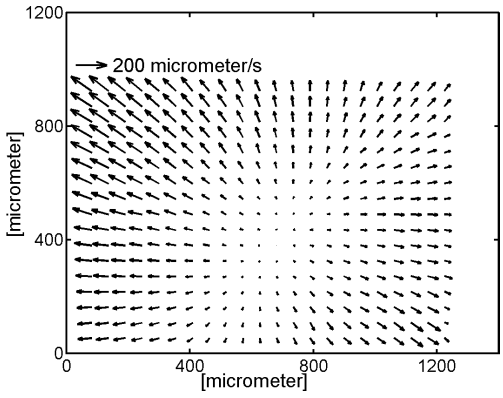

Figure 2. Streaming field in the nodal plane of λ/2 cylindrical mini-chamber; 1.38 MHz, 520 kPa.

In order to further estimate how the experimental results correlate with Rayleigh's micro-streaming analysis, the velocities obtained in the experiment were compared to the average streaming velocity in a nodal plane calculated with the Rayleigh model [1,3]. The velocity values at the border of the field of view were extrapolated to the distance where, according to the Rayleigh theory, the average streaming velocity is reached (0.9 mm from the central source point in the

present work). As Table 1 shows, the experimental velocity is quantitatively of the same order of magnitude as the calculated average Rayleigh micro-streaming velocity.

Table 1: Experimental and calculated streaming velocity

Sound pressure, kPa	Average Rayleigh streaming velocity, μm s^{-1}	Experimental streaming velocity, μm s^{-1}
380	35	86
450	50	116
520	66	166

Apparently, even though the assumptions made by Rayleigh for his model were not fully met in this experiment, it is still reasonable to use the model as a guide.

Cylindrical chamber with variable depth

According to the electrical admittance measurement, resonance in the chamber occurred at 1.43 MHz and 1.47 MHz for 0.5 mm (λ/2) and 0.25 mm (λ/4) channel depths, respectively.

At the channel depth of 0.5 mm, 1.0 μm particles concentrated mainly in the central plane of the chamber, where a pressure node was expected to occur, without a regular pattern. Vortices observed in the chamber included a rotating ring about 5 mm in diameter and counter-rotating vortex pairs of 0.35–0.55 mm at a distance of 150–200 μm from the base of the chamber. An increase in the pressure amplitude led to the distortion of the 5 mm diameter ring, the appearance of intensive eddies and precession of the particles.

At a 0.25 mm channel depth, the majority of 1.0 μm particles concentrated near the inner surface of the glass reflector, where a pressure node plane was expected to be. Numerous "potential wells", to which the particles were driven and formed clumps eventually, worked immediately on ultrasound application as the singular points of the vortices in which the particles streamed radially away from or towards their centres. A pattern similar to the one shown in Fig. 2 was observed in some areas. In the adjacent regions the vortices counter-rotated and the particles moved from the periphery of the area to its centre and then towards the base of the chamber.

Rectangular chamber

Several resonant peaks appeared in the electrical admittance spectra of the chamber. Experiments were carried out at a resonance frequency in the range 2.84 – 2.87 MHz, which is close to the transducer's thickness resonance (3 MHz). The particle distribution shows a pattern consistent with a complex acoustic pressure distribution. For each of the three channel depths used, (130, 170 and 270 μm), the 1.0 μm diameter latex beads concentrated in many small clumps in two layers when ultrasound was applied. One layer was near the glass reflector and another - at some distance from the chamber's base. The typical distance between the clumps in horizontal planes was 0.3 – 0.6 mm. The clumps were completely formed within 20 s of sound application. The region beyond the boundaries of the transducer's active radiation area had no regular pattern and was least affected by ultrasound. The observed patterns described above apparently originated from the non-uniformity of the acoustic pressure distribution within the active radiation area. Numerous pressure nodes resulted in many "potential wells", to which particles were driven and concentrated.

Streaming vortices were also observed in the chamber at a distance of 1/3 to 1/2 of the channel's depth from the base of the chamber. 1.0 μm latex beads, following the streaming in the vortices, produced several types of pattern, mainly spirals, rotating concentric rings and counter-rotating vortex pairs. The circulation of particles occurred in the planes parallel or at small angles to the transducer plane. The scale of the vortices ranged from 0.2 mm to 3–4 mm.

The particles in the vortices exhibited mainly two types of behaviour. The first case was vortex trapping, when the particles moved across the streamlines of the vortex and concentrated in the centre of rotation forming a clump, as shown in Figure 3.

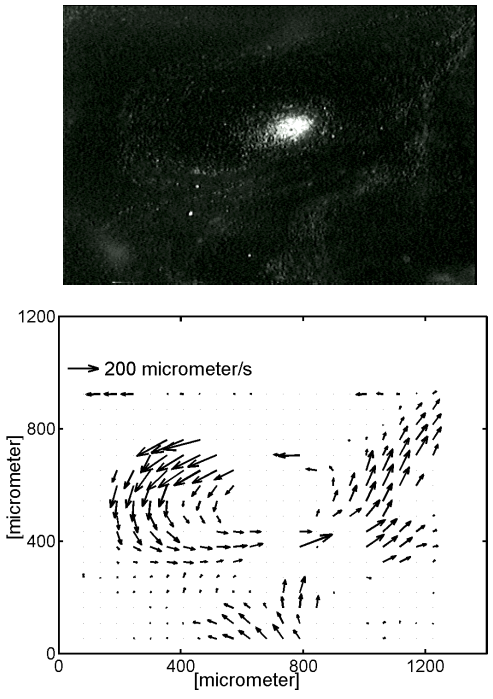

Figure 3. Microscopic image of vortex trapping and PIV results of the process; 2.89 MHz, 600 kPa; 38th s of sonication.

In the second case, the particles moved from the centre and formed a rotating ring, which gradually increased in diameter – Figure 4.

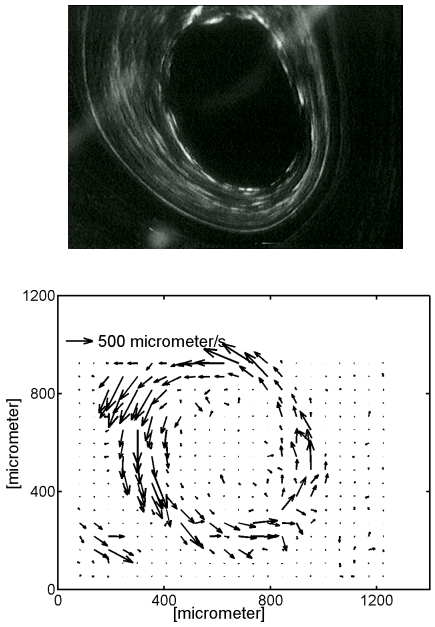

Figure 4. Microscopic image and PIV results of ring formation; 2.89 MHz, 600 kPa; 20th s of sonication.

Time independent flows in sonicated liquids have been extensively studied. Nyborg [10] has pointed out that in general a torque is exerted on any volume of a sonicated liquid even when the latter is homogeneous. The time averaged torque L on a spherical element about its centre is given by

$$L = (I/2\rho_o)\nabla \times F \qquad (1)$$

where I is the moment of inertia of the sphere about its centre, ρ_o is density and F is a force per unit volume. The magnitude of F and therefore of the torque depends only on the first order velocity *u* and tends to be large where *u* is non-uniform. e.g. near the edge of a beam or an edge of an obstacle in the field.

The 1.0 μm latex beads employed here to detect flow velocities by the PIV method reflect the distribution of velocity across the region where high torque vortices are present – Figures 3–4. However it is clear, since these small tracer particles become redistributed within the vortices as sonication continues, that they are experiencing significant forces within the vortex. Estimates were made of the centrifugal force operating on the particle and the Stokes drag on the particles that move across the streamlines. The tangential and radial components of the particles velocity were calculated from the analysis of video sequences and PIV results of ring formation at 310 and 600 kPa. A comparison of the two forces showed that the centrifugal force is many orders of magnitude too small to account for the movement of particles to the path of high particle concentration (Fig. 4). It is reasonable to assume that the mechanism of particles redistribution in the vortices originates from the non-uniformities in the acoustic pressure in the near field of the transducer.

Summary

Micro-particles distribution in short path length USSWs chambers was affected by acoustically induced streaming. The observed patterns included "Rayleigh"-type streaming, rotating concentric rings and counter-rotating vortex pairs. It is assumed that the acoustic pressure gradient determined the redistribution of particles in the vortices. The streaming contributes to the mass transfer in the chambers and is expected, together with DRF effects, to enhance micro-organisms capture rates in biosensors.

Acknowledgements

The authors are grateful to Sian Armstrong (admittance measurements) and Paul Malpas (PIV setup), School of Engineering, Cardiff University.

The work is supported by BBSRC (Research grant Nº 72/E17416).

References

[1] J.W.S.Rayleigh, The theory of sound, v.2. Dover publications, New York, 1945.

[2] L.P.Gor'kov, "On the forces acting on a small particle in acoustical field in an ideal fluid", Sov. Phys., vol.6, pp.773-775, 1962.

[3] J.F.Spengler, "Application of ultrasonic standing waves for suspending particle manipulation in the water industry", PhD Thesis, TU Berlin, 2002**.**

[4] L.K.Zarembo, in High-Intensity Ultrasonic Fields, L.D.Rozenberg (ed), Plenum Press New York, 1971.

[5] W.L.Nyborg, in Physical Acoustics, W.P.Mason (ed), v.2, Academic Press, New York, London, 1965.

[6] M.Raffel, C.Willert and J.Kompenhans, Particle image velocimetry: a practical guide, Heidelberg, Springer, 1998.

[7] E.H.Trinh and J.L.Robey, "Experimental study of streaming flow associated with ultrasonic levitation", Physics of Fluids, vol.6, pp.3567-3579, 1994.

[8] R.Liu, R.Lenigk, R.L.Druyor-Sanchez, J.Yang and P.Grodzinski, "Hybridization enhancement using cavitation microstreaming", Submitted to Journal of the American Chemical Society.

[9] X.Shi, R.W.Martin, S.Vaezy and L.A.Crum, "Quantitative investigation of acoustic streaming in blood", Journal of the Acoustical Society of America, vol.111, pp.1110-1121, 2002

[10]W.L.Nyborg, in Ultrasound: its application in medicine and biology, F.J.Fry (ed), Elsevier, Amsterdam, 1978.